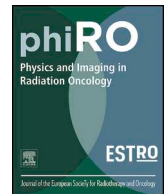




ELSEVIER

Contents lists available at ScienceDirect

Physics and Imaging in Radiation Oncology

journal homepage: www.elsevier.com/locate/phro

Original Research Article

Reconstruction of the electron source intensity distribution of a clinical linear accelerator using in-air measurements and a genetic algorithm

Egor Borzov^{a,*}, Alexander Nevelsky^a, Raquel Bar-Deroma^a, Itzhak Orion^b^a Department of Radiotherapy, Division of Oncology, Rambam Health Care Campus, Haifa 32000, Israel^b Department of Nuclear Engineering, Ben-Gurion University of the Negev, Beer Sheva 84105, Israel

ARTICLE INFO

Keywords:

Electron source intensity distribution
Focal spot
Genetic algorithm
Small field dosimetry

ABSTRACT

Background and purpose: The electron source intensity distribution of a clinical linear accelerator has a great influence on the calculation of output factors for small radiation fields where source occlusion by the collimating devices takes place. The purpose of this study was to present a new method for the electron source reconstruction problem.

Materials and methods: The measurements were performed in-air using diode and 6 MV $1 \times 1 \text{ cm}^2$ photon field in flattening filter-free mode. In Monte Carlo simulation, an electron target area was divided into a number of square sub-sources. Then, the in-air doses in 2D silicon chip array were calculated individually from each sub-source. A genetic algorithm search was applied in order to determine the optimal weight factors for all sub-sources that provide the best agreement between simulated and measured doses.

Results: It was found that the reconstructed electron source intensity from a clinical linear accelerator has the two-dimensional elliptical double Gaussian distribution. The source intensity distribution consisted of two intensity components along the in-plane (x) and cross-plane (y) directions characterized by full width half-maximum (FWHM): $\text{FWHM}_{x1} = 0.27 \text{ cm}$, $\text{FWHM}_{x2} = 0.08 \text{ cm}$, $\text{FWHM}_{y1} = 0.24 \text{ cm}$, $\text{FWHM}_{y2} = 0.06 \text{ cm}$, where broader components are 81% and 53% of the total intensity along x and y axis respectively.

Conclusions: The obtained results demonstrated an elliptical double Gaussian intensity distribution of the incident electron source. We anticipate that the proposed method has universal applications independent of the type of linear accelerator, modality or energy.

1. Introduction

Small photon fields are often used in the delivery of stereotactic radiosurgery (SBRT/SRS) treatments. Consequently, an accurate dosimetry of small fields is an important part of a medical linear accelerator characterization since it has an effect on calculations of the dose distribution in treatment planning systems (TPSs). Because the standard measurement procedure is not suitable for small-field dosimetry, the commissioning and verification of small-field dosimetry remains a challenging task for medical physicists [1]. To overcome the challenges of small-field dosimetry, many authors have proposed Monte Carlo (MC) methods as the best suitable tool for small-beam commissioning. To formalize the use of MC methods in small and nonstandard field dosimetry, Alfonso et al. [2] proposed a procedure to calculate the correction factors for specific combinations of the machine, field and type of detector. Obviously, a MC simulation must be extremely accurate and take into account all details, such as the machine and detector

dimensions and materials.

In the past decades, the EGSnrc MC code has been extensively tested and accepted as a gold standard in photon and electron beam dosimetry. The physical and chemical parameters of the components required for a MC model can be obtained from the manufacturer and are usually known with satisfactory accuracy. However, there are parameters that can be only estimated by the manufacturer: the energy and spot size of the incident electron beam which impacts the target surface. These values are necessary for a correct simulation of the bremsstrahlung generation in a linac treatment head. Moreover, the proper incident electron beam size has a great influence on the calculation of output factors for small radiation fields where source occlusion by the collimating devices takes place [3].

Notwithstanding, the first estimation of the electron parameters given by a manufacturer can be further improved following the approach proposed by Sheikh-Bagheri and Rogers [4]. This method is usually performed under assumptions of the Gaussian type for both the

* Corresponding author at: HaAliya HaShniya St 8, Haifa, 3109601, Israel.

E-mail address: george.borzov@gmail.com (E. Borzov).

<https://doi.org/10.1016/j.phro.2019.11.010>

Received 12 August 2019; Received in revised form 24 November 2019; Accepted 25 November 2019

2405-6316/© 2019 The Author(s). Published by Elsevier B.V. on behalf of European Society of Radiotherapy & Oncology. This is an open access article under the CC BY-NC-ND license (<http://creativecommons.org/licenses/by-nc-nd/4.0/>).

energy and spatial distributions of the electron source and eventually provides satisfactory results in modeling for most radiotherapy needs.

However for small fields, even after careful MC modeling of an accelerator, a substantial difference can be observed between the simulated and measured profiles and output factors. The reason for this difference is the increasing influence of the incident electron beam size on the small-field characteristics [5]. This issue makes the classic Sheikh-Bagheri and Rogers procedure insufficient for small radiation field modeling. Based on previous publications, we can distinguish three possible ways to obtain an estimation of the electron source intensity distribution: (i) an experimental method with direct measurements; (ii) an improved Sheikh-Bagheri and Rogers method that includes a MC simulation of the detector response; and (iii) mathematical reconstruction methods.

The brief review of experimental works done before 2005 can be found in the Bush's et al. study [6]. Later in 2009, Scott et al. [7] performed MC modeling to quantify the effect of the electron focal spot size on the source occlusion and output factors and as a matter of principle stated that there is an absence of experimental methods for determining incident electron beam properties. Currently, there still remains a noticeable lack of corresponding experimental works on modern linacs.

The method proposed by Sheikh-Bagheri and Rogers can also be improved and applied for the MC simulations of small fields. Following the formalism for the small-field dosimetry introduced by Alfonso et al. [2], the proper MC modeling of a linear accelerator in conjunction with the modeling of a detector response can provide detector-specific correction factors. Exemplary studies were performed by Cranmer-Sargison et al. [8] and by Francescon et al. [9] for several detectors. The adjustment between the measured and simulated penumbra was made by searching for an appropriate value of the full width half-maximum (FWHM) of the electron source assuming a circular Gaussian shape in Cranmer-Sargison's work and a Gaussian elliptical shape in Francescon's work. One should note that the fine tuning search of the source parameters was not algorithmic and remained trial and error. Additionally, in both works, the measurements were performed in water, while it was demonstrated previously that the measurements of in-air profiles were more sensitive to the energy and spot size of the electron incident beam impacting the bremsstrahlung target due to in-phantom electron scattering [4,10].

A mathematical reconstruction approach was firstly applied by Bush et al. [6]. The electron source was subdivided into annular regions with unknown weight factors. The search of weight factors was algorithmic and the adjustment was made between a measured and a MC simulated diagonal profile excluding penumbra regions. The authors estimated an optimal FWHM of the electron source with an uncertainty of 0.01 mm. Again, the measurements were performed in water, the radial symmetry of the electron source shape was assumed and the detector was not considered in the MC simulation. Moreover, the proposed method was not benchmarked against a MC simulation with known electron intensity distributions.

The most recent work for an electron source reconstruction was published by Papaconstadopoulos et al. [11], who proposed using the maximum-likelihood expectation-maximization (MLEM) algorithm. The MLEM algorithm iteratively produced ray-traces photons from the source plane to the exit plane and extracted corrections based on photon fluence profile measurements. The photon fluence profiles were determined by film measurements in air for the smallest field. The authors benchmarked this method against MC simulations and postulated a 0.12 mm (FWHM) reconstruction accuracy of the incident electron source.

The aim of this study was to present an approach for the incident electron source reconstruction that (i) uses two-dimensional profiles of a small field measured in-air; (ii) includes a detector in the MC simulation; (iii) utilizes an algorithmic search for the electron source distribution of an arbitrary shape; and (iv) is benchmarked against MC

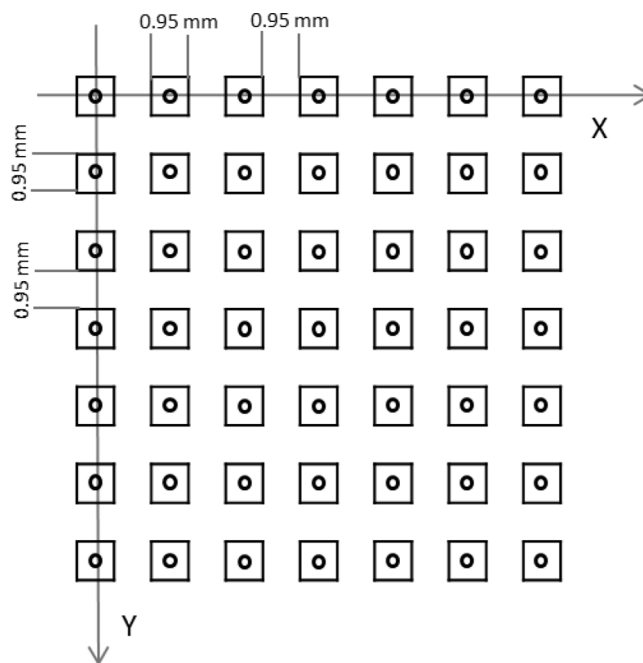


Fig. 1. Scheme of the SFD positions. Squares – positions of the SFD silicon chips during MC simulations. Circles – approximate positions of the center of the SFD detector during the measurements. All positions are placed equidistantly beginning from the center of the a $1 \times 1 \text{ cm}^2$ field.

simulations. The approach should support the selection of electron beam intensity distribution in the MC simulations aimed at modeling small fields and determining the detector-specific output factor corrections.

2. Materials and methods

2.1. Measurements

The Elekta VersaHD (Elekta AB, Sweden) linear accelerator equipped with the Agility MLC was used in this study. The in-air measurements were performed in a water phantom (MP3, PTW, Freiburg, Germany) using a stereotactic field diode (SFD; IBA Dosimetry, Schwarzenbruck, Germany) for a 6 MV $1 \times 1 \text{ cm}^2$ photon field in flattening filter-free (FFF) mode at a source-to-detector distance of 100 cm. The measured data were obtained in the form of a 2D array in which each value corresponded to an in-air measurement in a certain position of the SFD, repeated 3 times and averaged. The 2D array dimensions were -11.4 mm to $+11.4 \text{ mm}$ in steps of 1.9 mm that provided 169 measurement points. The scheme of the SFD positions during the measurements is illustrated in Fig. 1.

2.2. Monte Carlo model

The BEAMnrc code package was used for MC purposes. The model for the Agility treatment head of the Elekta VersaHD linear accelerator was created and described in detail in our previous work [12]. Other detailed information regarding MC simulation parameters and linear accelerator model can be found in the Appendix A.

2.3. Leaf/Jaw positioning

In MC simulations, it is regular practice that multileaf collimator (MLC) and jaw positions undergo additional fine tuning to achieve better agreement with the field size (which is defined as the width at the 50% dose level) between the measured and simulated beams. However, we have to pay attention to the fact that the 50% dose level

position itself depends on the electron source parameters, particularly for small fields. This fact means that the leaves/jaws positions need to be defined independently from the electron source parameters. In our study, we used the following methodology. First, the size of the radiation field was obtained from linac's software where it was defined following the VersaHD leaves/jaws automatic calibration procedure utilizing electronic portal imager device (EPID). Then, the manufacturer data, representing the relation between the radiation field size at the isocenter plane and the corresponding physical leaf/jaw tip position, were utilized for the exact leaf/jaw positioning in the MC simulation.

2.4. Modeling of the SFD detector

Based on the work of Cranmer-Sargison et al. [13], the SFD diode can be approximated as a silicon chip. In all simulations, the silicon chip with dimensions of $0.95 \times 0.95 \times 0.5 \text{ mm}^3$ in the x, y and z directions was placed in a number of predefined positions and irradiated by the $1 \times 1 \text{ cm}^2$ field. The positions of the SFD detector during all simulations were exactly the same as during measurements and are illustrated in Fig. 1. Thus, the MC calculated data were also obtained in the form of a 2D array (in coincidence with the in-air measured 2D array), with each value corresponding to the dose calculated in the silicon chip in a certain position.

2.5. Modeling of the subsources

The possibility of the representation of an electron source as a weighted sum of its subsources was demonstrated by Bush et al. [6]. In our study, we divided an electron target area of $4.8 \times 4.8 \text{ mm}^2$ into a number of square elements of two sizes: $0.2 \times 0.2 \text{ mm}^2$ (in the center region) and $0.4 \times 0.4 \text{ mm}^2$ (in the peripheral region). Then, each element was treated as an independent electron subsource characterized by certain (x,y) coordinates on the target surface, with a uniform spatial intensity distribution and energy distribution described in Section II.B.1. Since the linac geometry has two axes of symmetry, it was sufficient to simulate only one quarter of the subsources, including the subsources on the x- and y-axes, as illustrated in Fig. 2.

2.6. Source reconstruction, benchmarking and fitting

Once the simulated doses from each subsource were obtained, the reconstruction of the electron source intensity distribution was performed. The reconstruction was based on the search of the subsource weight factors minimizing the least-square cost-function:

$$\text{CostFunction} = \sum_V (A_V^{\text{meas}} - A_V^{\text{MC}})^2,$$

where A_V^{meas} is the dose at position V in the isocenter plane of the 2D array of the measured doses and A_V^{MC} is the dose at the same position V in the 2D array of the MC calculated doses. In turn, A_V^{MC} was defined as a weighted sum of the MC calculated doses in position V:

$$A_V^{\text{MC}} = \sum_{(x,y)} W(x,y) \cdot A_V^{\text{MC}}(x,y),$$

where $W(x,y)$ is a weight factor for a subsource in the position (x,y) on the target surface and $A_V^{\text{MC}}(x,y)$ is a MC calculated dose from this (x,y) subsource.

The cost function minimization was performed using a genetic algorithm (GA) with 333 variables (number of sub-sources), uniform initial population (weight-factors of the sub-sources) and rank scaling function. After the GA optimization finished and the weight factor matrix was obtained (repeated 10 times and averaged), a curve fitting procedure was applied to find a 2D interpolating function describing the electron source intensity distribution.

To benchmark the proposed technique, the whole procedure was applied for the case of measured doses being replaced with MC

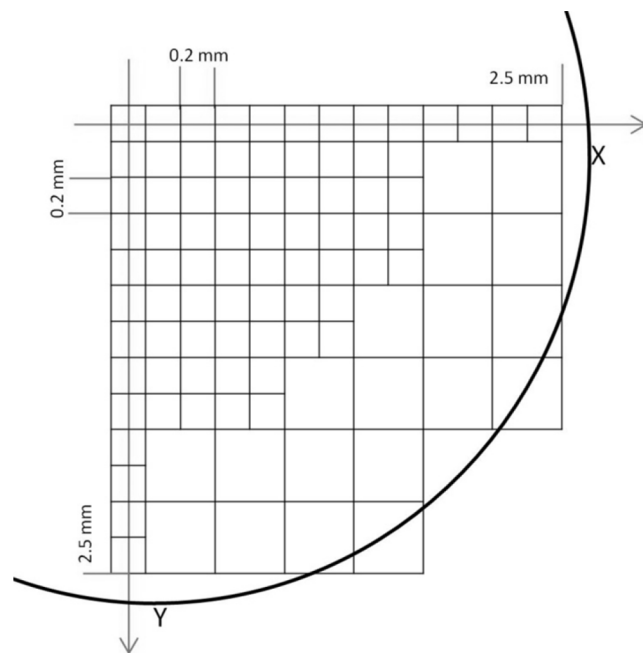


Fig. 2. Scheme of the target surface divided into subsources. The smaller squares are $0.2 \times 0.2 \text{ mm}^2$, and the larger squares are $0.4 \times 0.4 \text{ mm}^2$. The circle line represents the border of the high-Z alloy of the target insert, which serves to improve the photon production. Since a linear accelerator has two axes of symmetry, it is sufficient to model only one quarter of subsources, as demonstrated in the figure.

calculated doses obtained from the known electron source distribution. For benchmarking, the source intensity distributions were assumed to be either circular Gaussian with FWHM of 0.10 cm, 0.15 cm and 0.20 cm or elliptical Gaussian with the same as in our previous work parameters: $\text{FWHM}_x = 0.10 \text{ cm}$, $\text{FWHM}_y = 0.20 \text{ cm}$. It was reasonable to check the algorithm performance for these electron source parameters since we expected their proximity to the corresponding values of the real intensity distribution.

3. Results

The cross-plane and in-plane dose profiles from the measured in-air 2D dose array are presented in Fig. 3. The cross-plane and in-plane dose profiles from the MC simulated 2D dose array calculated in-air for the electron source distribution with $\text{FWHM}_x = 0.10 \text{ cm}$ and $\text{FWHM}_y = 0.20 \text{ cm}$ are also presented in Fig. 3 in order to demonstrate that such source parameters do not provide a sufficient agreement with the measured data. The same MC simulated 2D dose array was used to benchmark the performance of the proposed procedure to reconstruct the electron source intensity distribution. The weight factor matrix was successfully optimized and was fit to circular Gaussian sources (Eq. (B.1)) yielding FWHM of 0.11 cm, 0.16 and 0.21 cm and to the elliptical Gaussian source (Eq. (B.2)) yielding $\text{FWHM}_x = 0.11 \text{ cm}$ and $\text{FWHM}_y = 0.21 \text{ cm}$ (RMSE = 1.9%). Based on the achieved accuracy of the source distribution reconstructions, the benchmarking was considered successful.

After benchmarking, the whole procedure was applied to optimize the weight factor matrix of the electron source intensity based on the measured in-air 2D dose array. Then, the fit was performed with the two-dimensional elliptical Gaussian function (Eq. (B.2)): $\text{FWHM}_x = 0.10 \text{ cm}$, $\text{FWHM}_y = 0.16 \text{ cm}$, and root-mean-square error (RMSE) 6.1%. Since the goodness of curve fit was not sufficiently accurate, the fitting process was continued. A much better fit was obtained for the two-dimensional elliptical double Gaussian function (Eq. (B.3)): $A = 0.81$, $B = 0.53$, $\text{FWHM}_{x1} = 0.27 \text{ cm}$, $\text{FWHM}_{x2} = 0.08 \text{ cm}$,

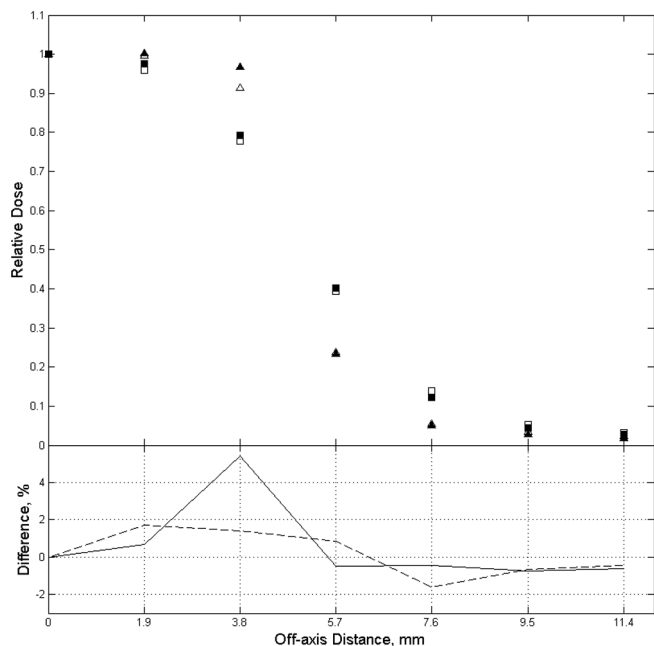


Fig. 3. The in-air measured (empty triangles – cross-plane, empty squares – in-plane) and simulated (filled triangles – cross-plane, filled squares – in-plane) doses; the MC simulated doses were calculated from the electron source distribution with $\text{FWHM}_x = 0.10$ cm and $\text{FWHM}_y = 0.20$ cm. Lines show relative local difference between the simulated dose and the measured dose (solid line – cross-plane, dotted line – in-plane).

$\text{FWHM}_{y1} = 0.24$ cm, $\text{FWHM}_{y2} = 0.06$, and $\text{RMSE} = 2.7\%$.

The reconstructed weight factor matrix of the electron source intensity distribution is presented in Fig. 4 in the form of a grayscale heat map which visually demonstrates that the source has two axes of symmetry and long low-intensity tails. The reconstructed matrix is shown as a 3D point distribution in Fig. 5 (upper) and intensity profiles along the x and y axes with the fitting curves from Eq. (2) in Fig. 5 (lower) where the perfect fit of the elliptical double Gaussian can be observed.

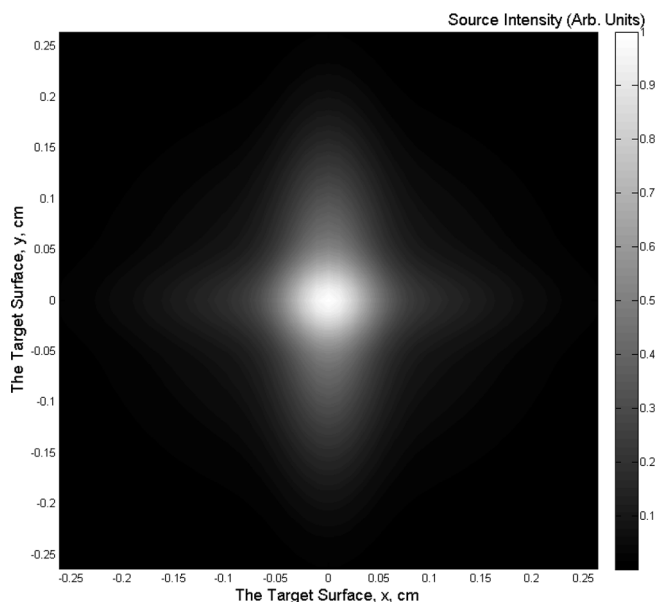


Fig. 4. Grayscale image of the reconstructed electron source intensity distribution.

4. Discussion

In the current study, we proposed a new method for the reconstruction of the electron source intensity distribution. The method includes in-air dose profile measurements, MC modeling of the linear accelerator and the SFD detector, and source reconstruction using optimization search with a genetic algorithm. An optimization search was performed without any assumptions about the electron source intensity distribution. Additionally, the algorithm performance was benchmarked against MC simulations with a known source distribution. The reconstruction was applied for the Elekta VersaHD linac, for which the electron source distribution was evaluated for the first time. Since small-field dosimetry is usually associated with SRS treatments that are delivered with the high-dose-rate FFF mode, the work was performed for a 6 MV FFF beam. There is no fundamental obstacle to applying the same procedure for other energies or modalities. The proposed method is general and allows reconstruction of the electron source distribution of any arbitrarily form for any linear accelerator.

Through the benchmark process, it was demonstrated that the reconstructed FWHM of the electron source overestimated the expected FWHM by approximately 0.01 cm in both the x- and y-axis directions. Most likely, this can be explained by the electron beam blurring occurring in the target. This observation agrees with the work performed by Sterpin et al. [14], which describes a broadening of the electron beam up to 0.04 mm for a similar incident energy within 0.13 mm of the target. The same effect was observed and discussed by Papaconstadopoulos et al. [11]. In fact, this demonstrates that the proposed algorithm reconstructs a shape that is closer to the X-ray spot distribution instead of the electron source distribution.

The double-Gaussian character of the electron source intensity has been observed and reported previously. In the work performed by Chen et al. [15], the authors used a slit-collimator method to experimentally obtain the X-ray source intensity distribution of the TomoTherapy system. They found that the source consisted of one Gaussian with a 0.075 cm FWHM and 72% peak amplitude and a second Gaussian with 0.227 cm FWHM and 28% peak amplitude. These values are rather similar to the corresponding parameters that were found in our work. We must emphasize that this two-component distribution should not be mistaken as the “focal” and “extrafocal” components of the X-ray radiation. The term “extrafocal” radiation is related to the fraction of the X-ray radiation reaching the measurement plane as a result of scattering processes in the linac’s head and is therefore characterized by a low intensity and broad distribution. A perfect illustration of such observations can be found in the work performed by Sham et al. [5]. The physical nature of the double-Gaussian distribution of the electron source remains unclear. This can most likely be explained by the electron cloud diffusion during beam travelling along the linac bending magnets.

Based on Chen et al. [15] study, Doerner et al. [16] performed their work to check the influence of the double-Gaussian source model on small-field dosimetry. For this purpose, the authors implemented the model into the BEAMnrc code and proved that it provided better agreement between the MC simulation and the measurements (via the Siemens PRIMUS linac). They found that the source model produced the largest influence on the relation between the calculated output factor and field size due to the occlusion effect. This emphasizes the importance of the correct source model utilized in the TPS, especially during SRS treatment planning.

We minimized the random experimental uncertainties by measurement repetitions, while the optimization uncertainties were minimized by multiple optimization runs. However, the accuracy of the source reconstruction includes other uncertainties that could not be fully eliminated. For example, bremsstrahlung X-ray production is very sensitive to the target material composition and its thickness. The second example is the limitation in the leaf/jaw positioning accuracy. Therefore, the final GA optimization results include the measurement

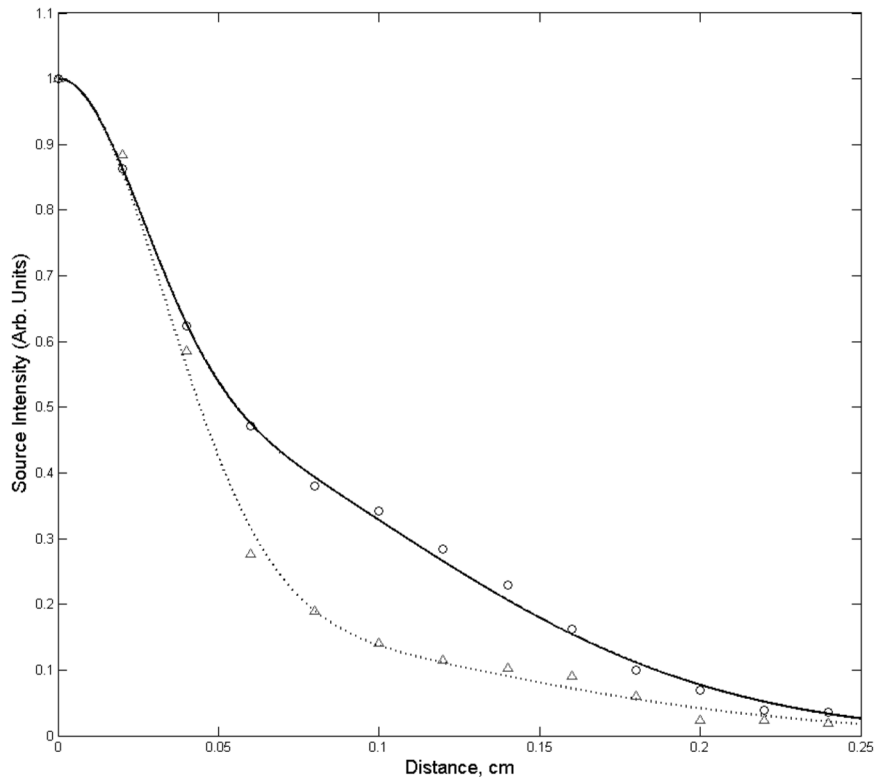
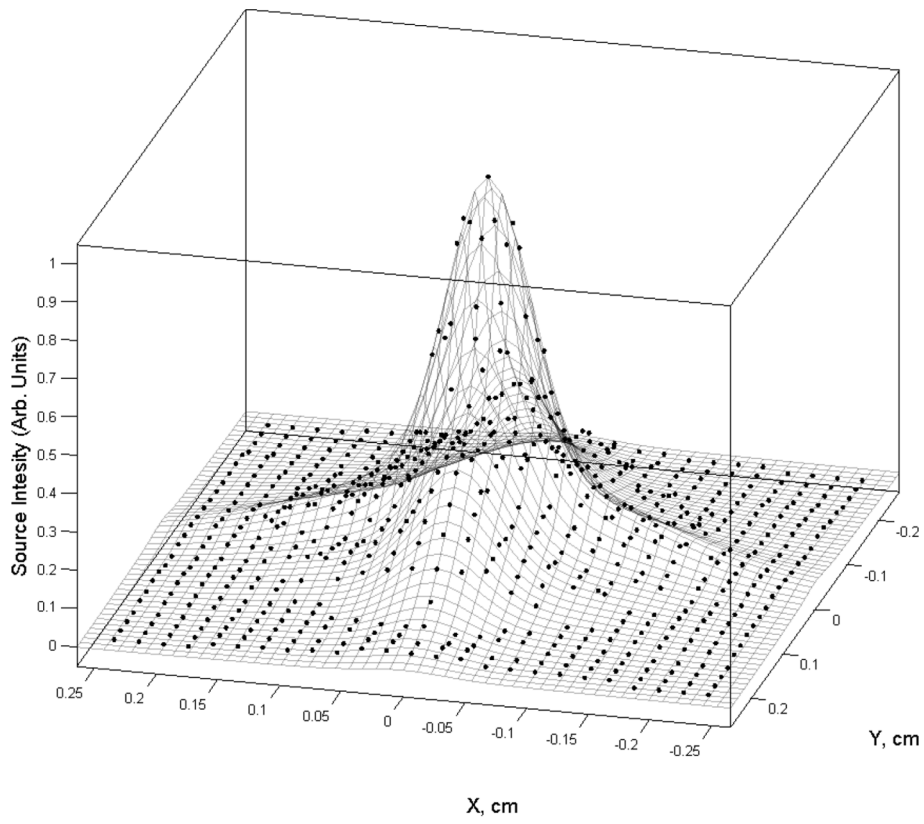


Fig. 5. The optimized electron intensity 3D curve (upper) and profiles along the x- and y-axis (lower) of the optimized electron source intensity distribution. The triangles (circles) are optimized weight factors along the x (y) axis; the solid (dotted) line is the fitted curve based on the two-dimensional double Gaussian function (Eq. (2)).

uncertainties mentioned above as well as the MC statistical calculation uncertainties. Finally, we can estimate the accuracy of the proposed method to be approximately 0.01 cm for the FWHM resulting from the benchmarking process.

During this study, an experimental work dedicated to the definition of the X-ray beam spot parameters was published by Jeung et al. [17]. The authors measured an “X-ray beam spot (where the electron beam strikes the target)” for Varian linear accelerator using self-made a dual-edge apparatus attached to the linac’s head and the electronic portal imaging device. The achieved distribution was successfully fit to a two-dimensional elliptical single Gaussian with FWHMs of about 1.6 mm. At the same time, in the recently published work by Papaconstadopoulos et al. [18] the reconstructed source distribution for the same linac model presented systematic deviations from a simple Gaussian distribution, mostly in the lower tail region, and double Gaussian functional form improved modeling the source in this region. These observations are in good agreement with the results of our study.

The electron source parameters obtained by different authors for various machines are quite straggled. Some difficulties are still present when trying to distinguish between the electron source size and the

focal spot size and in the definition (the origin and the magnitude) of the so-called ‘extrafocal radiation’. The authors suggest that the experimental definition of the electron source size of the Elekta Versa HD linac would add confidence to the results observed in the current study.

In conclusion, we proposed a new method for the reconstruction of the incident electron source intensity distribution for a clinical linear accelerator without any assumptions regarding the character of its distribution. The method utilizes a number of MC simulations that include SFD modeling and a simple experimental setup. The optimization was performed using a genetic algorithm that showed good performance for this task. The obtained results demonstrated an elliptical double Gaussian intensity distribution of the incident electron source. We anticipate that the proposed method has universal applications independent of the type of linear accelerator, modality or energy.

Declaration of Competing Interest

The authors declare that they have no known competing financial interests or personal relationships that could have appeared to influence the work reported in this paper.

Appendix A

The Monte Carlo parameters and Linear Accelerator Model

The BEAMnrc code was compiled as a shared library to avoid the use of correlated phase-space file data and large disk space. The transport parameters of the PCUT, ECUT and boundary crossing algorithm (BCA) were set to 0.010 MeV, 0.700 MeV (0.521 MeV for the in-phantom part) and EXACT, respectively. The EXACT BCA is an important parameter for the correct particle transport through the collimation components of the linear accelerator since it defines the shape of the dose profiles in the penumbra region. The bremsstrahlung cross-section enhancement with a splitting factor of 1000 in the target materials was applied to improve photon production. Directional bremsstrahlung splitting in conjunction with Russian roulette was applied with parameter selection based on recommendations published by Kawrakow et al. [19]. The number of initial particles in each simulation was selected so that the dose uncertainty in the silicon chips did not exceed 1% (one standard deviation) for the “out-of-field” chips, corresponding to approximately a dose uncertainty of 0.2% (one standard deviation) for “in-field” chips. The model for the Agility treatment head of the Elekta VersaHD linear accelerator was created and described in detail in our previous work [13]. In that work, the incident electron source parameters were adjusted following the approach of Sheikh-Bagheri and Rogers [4]. The mean electron energy of the 6 MV FFF beam was found to be 7.4 MeV with a FWHM of 0.5 MeV. The intensity of the spatial distribution was assumed to have the two-dimensional elliptical Gaussian form. The values of the FWHM for the cross-plane and in-plane directions ($FWHM_x$ and $FWHM_y$) were searched using a 0.05 cm step and were found to be 0.10 cm and 0.20 cm, respectively. The appendices model demonstrated very good agreement with the measured PDD and lateral dose profiles both for the MLC-based square fields and for the stereotactic conical applicators. However, the accuracy of the small-field corrections of the output factors for the SFD detector obtained in that work has been questioned since the electron source parameters were found using trial and error with a pre-assumed spatial distribution.

Appendix B

The Functional Forms used for fitting procedure

The simple circular Gaussian function:

$$f(x, y) = e^{-4 \cdot \ln 2 \cdot \left(\frac{x}{FWHM_x}\right)^2}, \quad (B.1)$$

The two-dimensional elliptic Gaussian function:

$$f(x, y) = e^{-4 \cdot \ln 2 \cdot \left(\frac{x}{FWHM_x}\right)^2} \cdot e^{-4 \cdot \ln 2 \cdot \left(\frac{y}{FWHM_y}\right)^2} \quad (B.2)$$

The two-dimensional elliptical double Gaussian function:

$$F(x, y) = \left(A \cdot e^{-4 \ln 2 \cdot \left(\frac{x_1}{FWHM_{x1}}\right)^2} + (1 + A) \cdot e^{-4 \ln 2 \cdot \left(\frac{x_2}{FWHM_{x2}}\right)^2} \right) \cdot \left(B \cdot e^{-4 \ln 2 \cdot \left(\frac{y_1}{FWHM_{y1}}\right)^2} + (1 - B) \cdot e^{-4 \ln 2 \cdot \left(\frac{y_2}{FWHM_{y2}}\right)^2} \right), \quad (B.3)$$

References

- [1] Das LJ, Ding GX, Ahnesjö A. Small fields: nonequilibrium radiation dosimetry. *Med Phys* 2008;35:206–15.
- [2] Alfonso R, Andreo P, Capote R, Huq MS, Kilby W, Kjäll P, et al. A new formalism for reference dosimetry of small and nonstandard fields. *Med Phys* 2008;35:5179–86.
- [3] Scott AJ, Nahum AE, Fenwick JD. Using a Monte Carlo model to predict dosimetric properties of small radiotherapy photon fields. *Med Phys*. 2008;35:4671–84.
- [4] Sheikh-Bagheri D, Rogers DW. Sensitivity of megavoltage photon beam Monte Carlo simulations to electron beam and other parameters. *Med Phys* 2002;29:379–90.
- [5] Sham E, Seuntjens J, Devic S, Podgorsak EB. Influence of focal spot on characteristics of very small diameter radiosurgical beams. *Med Phys* 2008;35:3317–30.
- [6] Bush K, Zavgorodni S, Beckham W. Inference of the optimal pretarget electron beam

- parameters in a Monte Carlo virtual linac model through simulated annealing. *Med Phys* 2009;36:2309–19.
- [7] Scott AJ, Nahum AE, Fenwick JD. Monte Carlo modeling of small photon fields: quantifying the impact of focal spot size on source occlusion and output factors, and exploring miniphantom design for small-field measurements. *Med Phys* 2009;36:3132–44.
- [8] Cranmer-Sargison G, Weston S, Evans JA, Sidhu NP, Thwaites DI. Implementing a newly proposed Monte Carlo based small field dosimetry formalism for a comprehensive set of diode detectors. *Med Phys* 2011;38:6592–602.
- [9] Francescon P, Cora S, Cavedon C. Total scatter factors of small beams: a multi-detector and Monte Carlo study. *Med Phys* 2008;35:504–13.
- [10] Tonkopi E, McEwen MR, Walters BR, Kawrakow I. Influence of ion chamber response on in-air profile measurements in megavoltage photon beams. *Med Phys* 2005;32:2918–27.
- [11] Papaconstadopoulos P, Levesque IR, Maglieri R, Seuntjens J. Direct reconstruction of the source intensity distribution of a clinical linear accelerator using a maximum likelihood expectation maximization algorithm. *Phys Med Biol* 2016;61:1078–94.
- [12] Borzov E, Nevelsky A, Bar-Deroma R, Orion I. Dosimetric characterization of Elekta stereotactic cones. *J Appl Clin Med Phys* 2018;19(1):194–203.
- [13] Cranmer-Sargison G, Weston S, Evans JA, Sidhu NP, Thwaites DI. Monte Carlo modelling of diode detectors for small field MV photon dosimetry: detector model simplification and the sensitivity of correction factors to source parameterization. *Phys Med Biol* 2012;57:5141–53.
- [14] Sterpin E, Chen Y, Lu W, Mackie TR, Olivera GH, Vynckier S. On the relationships between electron spot size, focal spot size, and virtual source position in Monte Carlo simulations. *Med Phys* 2011;38:1579–86.
- [15] Chen Q, Chen Y, Chen M, Chao E, Sterpin E, Lu W. A slit method to determine the focal spot size and shape of TomoTherapy system. *Med Phys* 2011;38:2841–9.
- [16] Doerner E, Caprile P. Implementation of a double Gaussian source model for the BEAMnrc Monte Carlo code and its influence on small fields dose distributions. *J Appl Clin Med Phys* 2016;17:212–21.
- [17] Jeung A, Zhu L, Cassese M, Luevano R, Star-Lack J. Dual edge apparatus and algorithm for measurement of x-ray beam spot parameters. *Med Phys* 2018;45:5080–93.
- [18] Papaconstadopoulos P, Levesque IR, Aldelajjan S, O'Grady K, Devic S, Seuntjens J. Modeling the primary source intensity distribution: reconstruction and inter-comparison of six Varian TrueBeam sources. *Phys Med Biol* 2019;64:135005.
- [19] Kawrakow I, Rogers DW, Walters BR. Large efficiency improvements in BEAMnrc using directional bremsstrahlung splitting. *Med Phys* 2004;31:2883–98.